

ANNALS OF THE NEW YORK ACADEMY OF SCIENCES

Issue: *Critical Contributions of the Orbitofrontal Cortex to Behavior***Population coding and neural rhythmicity in the orbitofrontal cortex**Cyriel M.A. Pennartz,^{1,2} Marijn van Wingerden,^{1,3} and Martin Vinck¹¹Cognitive and Systems Neuroscience, Center for Neuroscience, Swammerdam Institute for Life Sciences, Faculty of Science, ²Cognitive Science Center Amsterdam, University of Amsterdam, Amsterdam, the Netherlands. ³Department of Comparative Psychology, Institute of Experimental Psychology, Heinrich-Heine University Düsseldorf, Düsseldorf, Germany

Address for correspondence: Dr. Cyriel M.A. Pennartz, Cognitive and Systems Neuroscience Group, Center for Neuroscience, Swammerdam Institute for Life Sciences, Faculty of Science, University of Amsterdam, Sciencepark 904, 1098 XH, Amsterdam, the Netherlands. c.m.a.pennartz@uva.nl

The orbitofrontal cortex has been implicated in the prediction of valuable outcomes based on environmental stimuli. However, it remains unknown how it represents outcome-predictive information at the population level, and how it provides temporal structure to such representations. Here, we pay attention especially to the population coding of probabilistic reward, and to the importance of orbitofrontal theta- and gamma-band rhythmicity in relation to target areas. When rats learned to associate odors to food outcome with variable likelihood, we found single-cell and population coding of reward probability, but not uncertainty. In related experiments, reward anticipation correlated to firing activity locking to theta-band oscillations. In contrast, gamma-band activity was associated with a firing-rate suppression of neurons that was most active during goal-directed movement. Orbitofrontal coding of outcome-relevant parameters appears bound to all relevant temporal phases of behavioral tasks, has a distributed nature, and is temporally structured according to multiple modes of rhythmicity.

Keywords: phase locking; population coding; probability; reward; synchrony; uncertainty

Introduction

While the exact cognitive functions of the orbitofrontal cortex (OFC)—and especially its various subregions—are still enigmatic, accumulating evidence suggests a main role in the adaptation of previously acquired behaviors. Mechanistically, this adaptation may be caused by an updating of representations that predict outcomes based on stimuli and actions.^{1–4} In these adaptive processes, the OFC interacts with a network of connected brain structures, including the amygdala, medial prefrontal cortex, dorsal and ventral striatum, and monoaminergic cell groups in the mesencephalon and brain stem.^{5,6} Using a disconnection procedure, for instance, Baxter *et al.*¹ showed that communication between orbitofrontal cortex and amygdala was required for monkeys to adapt their choice behavior when the outcome value of their actions was reduced.

Another well-known paradigm in which OFC lesions are known to have a strong impact is reversal learning. When, after the initial acquisition of stimulus–outcome contingencies, the pairings are reversed so that a previously rewarded stimulus is now coupled to a negative outcome, and the previously negative stimulus is now paired with reward, rats and monkeys with OFC lesions are impaired, especially during the early reversal phase.^{7–9} Schoenbaum *et al.*³ recently dissected the pattern of deficits further and concluded that “the OFC is necessary for mobilizing information about the value of the expected outcome to guide or influence responding.” Updating of state–outcome associations probably takes place not only in the OFC, but also in other brain regions, such as the amygdala, working in concert with structures encoding errors in the prediction of future reward or punishment. An important observation is that devaluation of Pavlovian cues by illness or satiety is impaired by

OFC lesions in monkeys and rats, even when the OFC is still intact during the acquisition and devaluation procedure.^{10,11} This suggests that the OFC influences behavior by retrieving, maintaining, and/or using outcome value information at the time of decision making. A further role for the OFC may lie in the control over changes in downstream value-based representations, such as in the amygdala.¹² Recently, the adaptive function of the OFC was also specified in relation to components of learning that differ from pure stimulus-value updating (e.g., the assignment of “credit” or causal responsibility for obtaining reward to particular choices).¹³

However, it has remained enigmatic how OFC representations of outcome properties, including value, are linked to effects on behavior: do these functions primarily help the organism to make accurate, up-to-date choices, or do they also exert effects on the speed and timing of behavioral responses? While there is mixed evidence concerning the causal importance of the OFC in behavioral inhibition,^{14–17} we will revisit the issue of inhibition and response timing from a neurophysiological perspective.

Despite incremental insights in the behavioral and cognitive functions of the OFC, we likewise know little about the neural mechanisms operating to bridge the gaps between single-cell activity, population coding, and behavioral output. We do have a basic knowledge on how several outcome- and decision variables are coded at the single-neuron level (such as reward magnitude, delay to reward, effort required, and relative value of one presented stimulus vs. another).^{4,18–23} But how is cellular activity configured at the aggregate level of populations to generate mass output that is powerful enough to direct activity changes in target areas, such as the striatum and basolateral amygdala? In particular, the role of the OFC in coding probabilistic properties of outcomes is hotly debated, and it is largely unknown how OFC cell populations may code how probable or uncertain a possible outcome is, given a situation with multiple stimuli and actions of variable value.^{2,24}

A further topic of interest relates to the dynamic mode of activity used by OFC assemblies to code information. Whereas previous OFC studies embraced the classical approach of studying time-averaged firing rate as the central principle for neural coding, we asked whether also the tempo-

ral patterning of firing conveys information about outcome variables. The fine temporal structure of spike trains, studied in relation to mass rhythmicity as visible in local field potentials (LFPs), is likely to affect the impact of OFC output on target structures. If spike trains of different OFC pyramidal neurons are temporally aligned, their glutamatergic outputs converging on target cells will temporally summate more easily than when dispersed. The rhythmic phasing of OFC activity, relative to connected areas, may also affect the efficacy of their communication.^{25,26} Moreover, rhythmically synchronized spike output elicits coherent, temporally contiguous sequences of pre- and postsynaptic activity that have consequences for spike-timing-dependent plasticity.²⁷ Here we will first review the predictive neural coding of outcome variables such as reward probability, both at the single-cell and population level, and then discuss mechanisms for rhythmic synchronization in the OFC, especially in the theta and gamma frequency bands, and examine their functional consequences.

Methodology

We made ensemble recordings from rat orbitofrontal cortex using tetrode arrays (more specifically, from the ventral and lateral orbital areas, i.e., areas VO/LO).²⁸ With this technique, ensembles of up to 90 neurons can be recorded simultaneously, with single-unit resolution and jointly with LFP recordings.^{22,29,30} Recordings were made during various behavioral tasks, based on an odor discrimination design with Go/No-Go decisions (Fig. 1).^{31,32} Briefly, in each trial a rat typically samples an odor stimulus from an olfactory port in the conditioning chamber, retracts its snout from this port, and then executes a Go or No-Go decision. Trial onset is signaled by a cue light. The period between odor onset and snout retraction is labeled “odor period.” In the case of a Go decision, the rat walks over to a trough at the other side of the chamber (“movement period”), where it waits for a fixed amount of time (usually 1.0 or 1.5 sec) for the outcome to become available (“waiting” or anticipatory period). The “outcome period” starts directly after the waiting period and may comprise delivery of reward (sucrose solution or a food pellet, following the positive odor or S+) or a mildly aversive outcome (quinine solution, following the negative odor or S–), or the absence of any programmed

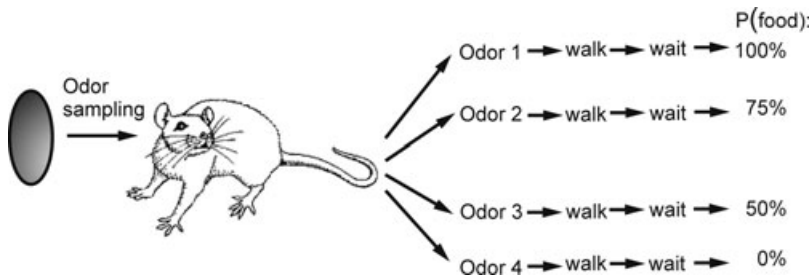


Figure 1. Behavioral paradigm for studying neural coding of reward probability. The spatial layout of the scheme follows the order of task phases from left to right: (i) odor sampling phase; (ii) Go or No-Go decision of the rat; (iii) in the case of a Go response, the rat responds to an odor by walking from the odor port to the food trough; (iv) on arrival at this trough, the rat waits for a defined period before a food pellet is or is not delivered. Each of the four odors applied in this task was associated with a distinct probability (P) of food delivery (0, 50, 75 or 100%). Although rats learned well to make a No-Go decision in response to the nonrewarded odor 4, the early trials of every session were marked by Go responses to every odor because at the start of every new session all odors were novel.

consequence (“zero outcome”). In the case of a No-Go decision, the rat retracts its snout from the port but does not continue to execute a response that would lead to outcome delivery otherwise. Typically, a set of odor stimuli is offered across different trials so that a subset of these stimuli is rewarding and another subset is coupled to a negative outcome or has no consequence. In the studies summarized below, all odors were novel at the onset of each new session; therefore, the animals were required to learn new odor–outcome pairings in every session. Importantly, rats were required to maintain their body positions, sustaining their nose pokes, both during the anticipatory period and the odor-sampling period (≥ 750 ms).

Coding of reward probability versus uncertainty

Coding of reward probability and uncertainty was studied in a task design with four distinct odor stimuli coupled to varying probabilities of food (0, 50, 75, or 100%; no aversive outcome condition was applied).³³ Analyzing the data at a single-neuron level, we first confirmed that all behavioral phases of the task were represented by firing correlates of OFC neurons. In agreement with previous studies, subsets of OFC cells typically generated firing increments selectively during the odor, movement, waiting, or outcome delivery periods (sometimes cells were found correlating to two task periods, but usually not more).^{18,32,34,35} This neural “tessellation” of task phases underscores that all phases of a behavioral sequence leading up to an outcome are represented in the OFC, with distinct phases coded

by different ensembles. We next studied whether firing patterns of neurons, in advance of outcome delivery, exhibited firing-rate correlations to different probabilistic outcome conditions. Of all cells with a significant firing-rate correlate to the movement and waiting periods of the task ($n = 78$ out of 541 cells recorded in total), 21.8% exhibited a significant modulation by the probability of future reward. In addition to a monotonic increase of firing rate with rising probability, we also found monotonic decrements or U -shaped relationships.³³

Although these firing patterns indicated single-cell sensitivity to probability, this analysis did not yet discriminate between coding of probability versus uncertainty. Here we refer to “uncertainty” as economic risk, quantified by the variance in probability distributions of reward value. We therefore grouped the responses from the two trial types with the two most certain outcomes (0 and 100%) together, contrasting them against the least certain outcome trials (50 and 75%). Only one out of 78 neurons significantly discriminated between these contrasting conditions. When, however, the high-probability trial types (75 and 100%) were contrasted against low-probability trial types (0 and 50%), no less than 17 out of the same 78 neurons (21.8%) were discriminatory. This fraction was significantly larger than the fraction discriminating on the basis of uncertainty ($P < 3.10^{-4}$).³³

Single-unit correlates are informative about the processing functions of a brain area under scrutiny, but it is often unclear whether the single-unit coding is powerful enough to affect the functioning of target areas in the face of population noise. A

single output from an OFC neuron reaching a target area may be overpowered by other OFC outputs uncorrelated to this single output (either in the sense of noise or because these outputs correlate to different task parameters). Using a population-coding approach called “template matching,”³⁶ we first examined whether reward probability could be decoded from OFC firing patterns during the movement and waiting period. Similar results were obtained using Bayesian coding. Population coding was significantly above chance level for varying sizes of ensembles contributing to the decoding procedure, indicating that reward probability was consistently represented in OFC population patterns. This was the case for the movement as well as the waiting period. Finally, we modified this approach and asked whether OFC population patterns were more consistent with coding of uncertainty or magnitude of probability. As in the single-cell approach, we found that population patterns characteristic of low-probability trials were much more similar to each other than to high-probability trials, whereas patterns with high certainty (100% and 0%) were highly dissimilar to each other.³³ In addition to confirming the single-cell findings, the population coding results indicated a distributed type of probability coding across OFC cell groups.

Altogether, these data show that OFC populations code an important outcome variable, namely the probability of obtaining a reward, during task stages where the animal anticipates the outcome either during locomotion or stationary waiting. Firing-rate modulations due to other outcome parameters such as reward magnitude²³ or delay to reward²¹ are also temporally distributed across the population of cells, giving rise to the concept of the OFC encoding a high-dimensional “matrix” of information, laid out according to task time (or “time until outcome”) along one axis and outcome variables (such as magnitude, delay, probability, sweetness) along other axes.

Because other recent recording studies^{37,38} have indicated neural correlates of uncertainty in the OFC, the question arises why our study did not reveal such coding in any robust way. Also recording from rat OFC, Kepecs *et al.*³⁷ used a very different task design, in which uncertainty pertained to the difficulty of discriminating odor mixtures, and reward probability was not parametrically varied as a function of stimulus identity. O’Neill and Schultz³⁸

recorded from macaques that were well trained on a cued saccadic eye movement task with risky outcomes, and one of the major differences with our study is that rats were learning new odor–outcome pairings every new session. Thus, one possible explanation of the difference, apart from species considerations, holds that when animals are in the midst of learning novel stimulus–outcome contingencies, the overall uncertainty is too large to allow a more detailed specification of stimulus-coupled uncertainty at the neural level, whereas such a specification might arise during further training on the same stimuli. Another difference is that O’Neill and Schultz visually cued the amount of risk to the monkey.

Theta-band synchronization

As discussed above, the OFC is thought to contribute to the flexible adjustment of behavior by enabling the modification of stimulus–outcome associations in other areas, such as the basolateral amygdala (BLA), with which it has strong reciprocal connections.^{3,12,39,40} Firing OFC cells transmit their signals to downstream areas, such as the ventral and dorsal striatum, ventral tegmental area, and substantia nigra pars compacta. OFC output may be used in these downstream areas in various ways. A first possible contribution holds that information on the expected value of outcome, coded by OFC projection neurons, reaches ventral tegmental dopaminergic cell groups to compute reward-prediction errors.^{41–45} Several computational variants of this idea are conceivable, but in general take OFC output to signal the value of predicted reward (e.g., a time-varying value signal (V_t), as applied in temporal difference-learning models.^{32,43,44,46,47} Subsequently, reward prediction errors coded by dopamine neurons may be instrumental in updating synaptic weights in target areas, such as striatum, amygdala, and medial prefrontal cortex. Experimental support for OFC coding of outcome-value information is strong (see above), but it is not yet known how this information is channeled to dopaminergic cell groups, or used in their computations. A second possibility holds that a subset of OFC neurons code reward-prediction errors itself.⁴⁵ Both the first and second function raise the possibility that OFC signals coding expected outcome may also operate in dopamine-independent reinforcement learning mechanisms, for instance

mediated by direct glutamatergic OFC projections to target areas such as the amygdala.^{48,49} This view of an interconnected cortico-subcortical network, involved in flexibly updating the current value associated with a stimulus, presupposes functionally efficacious connections between the partner areas.

Phase synchronization of slow (~1–12 Hz) rhythms in LFP oscillations between areas has been proposed as a functional mechanism for coupling areas that are anatomically distant.^{50–58} Strong coherence, in combination with a “good” phase relationship, may allow distant neuronal ensembles to interact, while taking conduction delays into account.^{25,26} In this context the “goodness” of the phase is indeed defined by the efficacy of communication. Womelsdorf *et al.*⁵⁹ argued that the key cognitive function supported by selective theta synchronization is the “structured retrieval of choice-relevant information around decision points,” and suggested that distributed theta oscillatory states in cortical networks are involved in successful retrieval of task-relevant representations of stimulus–outcome relationships and contextual rules. In addition, theta-band synchrony has been proposed to subserve the read-in and initial storage of information in higher sensory and associational areas, including the hippocampus.^{60,61} Here we investigated the role of theta-band synchrony in the temporal organization of OFC firing patterns in a behavioral task where sensory read-in, memory retrieval, decision making, and outcome anticipation all play a role, but in different phases of the task.

In a two-odor discrimination Go/No-Go task similar to the paradigm of Figure 1,^{22,32} Van Wingerden *et al.*⁶² showed that outcome-related information encoded by OFC single units in rats becomes highly synchronized to OFC theta oscillations in anticipation of reward. The anticipatory task phase marked by this high degree of theta synchronization is temporally situated after the animal made a Go/No-Go decision and locomotor response, and takes place when the rat is waiting for the outcome to become available.

Prominent theta oscillatory activity (peaking at 6 Hz) was recorded locally from the OFC using tetrodes, and about half of the recorded cells showed significant phase-locking to this rhythm (Fig. 2A, also see Refs. 63 and 64). This group of phase-locking cells is considerably larger than the subgroup expressing information about the expected

outcome in its firing rate. Single units were identified as coding expected outcome information by comparing their firing rate during the anticipatory period to a baseline period, and by verifying that this rate change was different for sucrose versus quinine-reinforced trials. In this anticipatory period, right before outcome delivery, these units showed strong spike-field phase locking to the local theta rhythm. This locking is manifested by the fact that single-neuron spikes consistently fire in a particular, narrow range of phases of the locally recorded theta oscillations. Spike-field phase locking was stronger when anticipating a positive (sucrose) rather than a negative (quinine) outcome, and increased in step with task acquisition as gauged by behavioral measures. No correlation was found between theta power or frequency and the rat’s licking frequency during the waiting period. Nonetheless, theta rhythmicity may be more globally correlated to sensorimotor activity in addition to outcome expectancy.⁶⁵ Separate experiments using 32-site silicon multi-channel probes with evenly spaced (100 μm) recording points, followed by current source density (CSD) analysis, indicated a local origin of theta rhythm in the orbitofrontal cortex, consistent with the fact that hippocampal theta is predominantly found during locomotion, which precedes the anticipatory period in our paradigm.⁶²

Strikingly, when the rule governing the cue–outcome contingencies was reversed, theta-band phase-locking in the OFC gradually collapsed across approximately the first 10 reversal trials in which the previously rewarded, but now negative odor was presented. When animals were learning the reversed contingencies, theta-band phase locking in the anticipatory period following the cue previously paired with quinine, but now with sucrose, became gradually prominent, also across the first ~10 trials (Fig. 2D). This suggests that theta-band phase locking does not carry “old reward” information for very long after the reversal has occurred.

Theta power during anticipation of reward, studied on a trial-by-trial basis, exhibited features of a value function reminiscent of temporal difference-learning types of model:^{46,66,67} at the end of task acquisition, a prominent theta oscillation was present from the onset of the waiting period until positive outcome delivery, but not before a negative outcome. Thus, it had a sustained nature, at least for the duration of the anticipatory period. When the

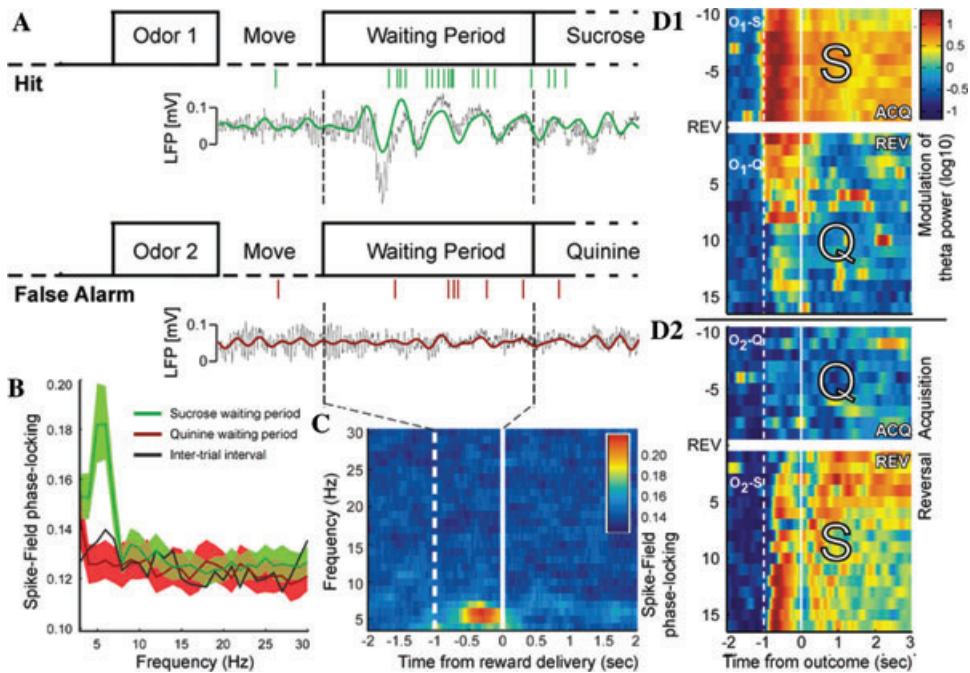


Figure 2. Theta-band synchronization in the OFC during reward expectancy. (A) Task outline with raw local field potential segments recorded during different task periods (black) and band-pass filtered LFP (4–12 Hz) (green trace, hit trial; red, false alarm trial) and spike trains from one unit, recorded on a different tetrode (vertical green/red bars). (B) Average spike-field phase-locking spectra during the waiting period, separated for sucrose and quinine trials, and during (unrewarded) inter-trial-interval fluid pokes. Shaded regions indicate 95% bootstrapped confidence intervals on the mean. (C) Time course of average (across all cells) phase-locking strength (in color) centered on reward delivery. Phase-locking was calculated in 500 ms symmetric windows centered on each time point. Solid line: reward delivery; dashed line: start of waiting period. (D) Trial-by-trial modulation of theta power (6 Hz) during acquisition and reversal. Rows represent consecutive trials from top to bottom, numbered relative to the onset of reversal learning (REV). Color scale indicates theta power modulation compared to baseline. Odor 1 (O_1) predicts sucrose (S) before reversal and quinine (Q) after reversal (D1). Odor 2 (O_2) predicts quinine before reversal and sucrose after reversal (D2). Dashed white line, start of waiting period; solid white line, fluid delivery; ACQ, acquisition. Adapted from Van Wingerden *et al.*⁶²

contingencies were reversed, the theta state persisted for a few trials in those trials initiated by a previously rewarded, but now negative cue, and then gradually faded (Fig. 2D1). In contrast, in trials where reward now followed the cue that previously predicted a negative outcome, theta synchrony started appearing. On the very first trials after reversal, when reward was highly unexpected, the theta state only appeared after reward delivery. However, as reversal learning proceeded, the theta state in these trials commenced progressively earlier, until settling at the start of the waiting period (Fig. 2D2). This backward shift in time, across trials, corresponds to a progressively earlier, experience-dependent computation of expected reward as predicted by temporal difference models. Further work is needed to examine whether this correspondence holds in detail.

These results indicate that outcome-relevant information is supported by a temporal code, operating in addition to rate coding in the OFC. Synchronized activity in the theta band has also been described in various target areas of the OFC, some of which may be involved in the computation of value functions, capturing net expected reward, and of reward prediction errors, such as the striatum and amygdala.^{51,68,69} Coherence between theta oscillatory states in different structures likely affects the efficiency of their communication, also by temporally structuring or driving gamma oscillations in local networks that can be found nested on theta oscillations, possibly adding extra synchronization to the ensemble activity.^{56,70} This flexible type of interaction may allow for the updating of synaptic weights, for example through

spike-timing-dependent plasticity processes in target structures.^{71,72}

In addition to theta oscillations, much effort has been put in understanding the significance of higher frequency rhythms such as gamma oscillations. Recent advances have underlined the importance of examining the relations between rhythms of different frequencies, within and across brain structures.^{73–75} Preliminary results from our group indicate that cross-frequency phase–amplitude coupling between theta and gamma rhythms exists in the OFC. We are currently investigating whether this phase–amplitude coupling correlates with measures of behavioral performance.

Gamma-band synchronization

A widespread phenomenon in the nervous system is gamma-band synchronization (30–90 Hz).^{76–87} Accumulating evidence suggests that gamma-band synchronization plays an important role in selective attention,^{26,81,88} can increase the speed and efficiency of information transmission,^{89–91} and subserves sensory coding and assembly formation.^{92–98} There is increasing consensus that gamma-band synchronization in cortical structures emerges from a recurrent interplay between pyramidal cells and fast spiking basket cells.^{57,79,99–103} Fast spiking basket cell activity is required for the emergence of gamma-band synchronization by entraining pyramidal cells.^{79,104,105} Yet it is debated whether pyramidal cells need to provide precisely timed, gamma-rhythmic inputs to fast spiking basket cells.^{57,79,101–103,105,106} In many sensory areas, gamma-band synchronization is induced by sensory stimuli.^{76,78,80,82,107–109} Yet much less is known about the characteristics of gamma-band synchronization in areas that subserve higher cognitive functions, such as the OFC.

We have recently shown that olfactory stimulation induces robust gamma-band synchronization (60–80 Hz) in the OFC of freely behaving rats (Fig. 3).¹¹⁰ A spectrally confined increase in gamma-band power was visible in the LFP spectrogram, and OFC spikes were strongly locked to the induced LFP gamma-band oscillations, falling on average around the peak of the oscillation (Fig. 3A). While the spectro-temporal characteristics of the induced OFC gamma-band synchronization appear similar to those found in visual cortex,^{111,112} we observed that OFC gamma-band synchronization

has two unique characteristics that set it apart from gamma-band synchronization observed in other brain areas. First, the occurrence of gamma-band synchronization was completely dependent on the acquisition of stimulus–outcome associations. Second, while gamma-band synchronization was induced by olfactory stimulation, it was exclusively expressed by a subset of cells, the activity of which was selectively enhanced during the subsequent movement phase and represented outcome value in this phase.

Rats performed a two-odor Go/No-Go discrimination task in which they acquired *de novo* stimulus–response associations every new session. Gamma-band synchronization was not induced by the first presentation of a novel odor but only emerged over trials (Fig. 3B and C). This increase in gamma-band synchronization over trials was especially strong in sessions where rats acquired stimulus–response associations rapidly. Hence, it was not a mere consequence of the repeated presentation of the same olfactory stimulus but reflected the acquisition of stimulus–response associations. While the strength of gamma-band synchronization was strongly correlated with learning, it increased similarly for the S+ and the S– conditions, that is, it did not contain information about stimulus identity or behavioral outcome (Fig. 3B and C). In contrast, gamma-band synchronization in visual cortex and at several stages of the olfactory system has been found to be strongly stimulus selective.^{95,107,113–116}

Gamma-band synchronization is often investigated as a population rhythm, that is, irrespective of differences in firing rate selectivity of cells for, for example, stimulus or action properties in the local population and by using multiunit activity or LFP signals. This approach may to some extent be valid for brain areas with a spatially homogeneous distribution of firing rates; however, there exists a great diversity in firing rate selectivity in the OFC. We have proposed that in structures with diverse responses such as the OFC, the flexible linking of cells into functional assemblies occurs through phase-synchronization to the same oscillation.¹¹⁰ One prominent class of cells in the OFC (“odor cells”) has firing rates that are modulated by olfactory stimulation and often differentiate between a given pair of olfactory stimuli (cf. Schoenbaum *et al.*³²). For these “odor cells,”

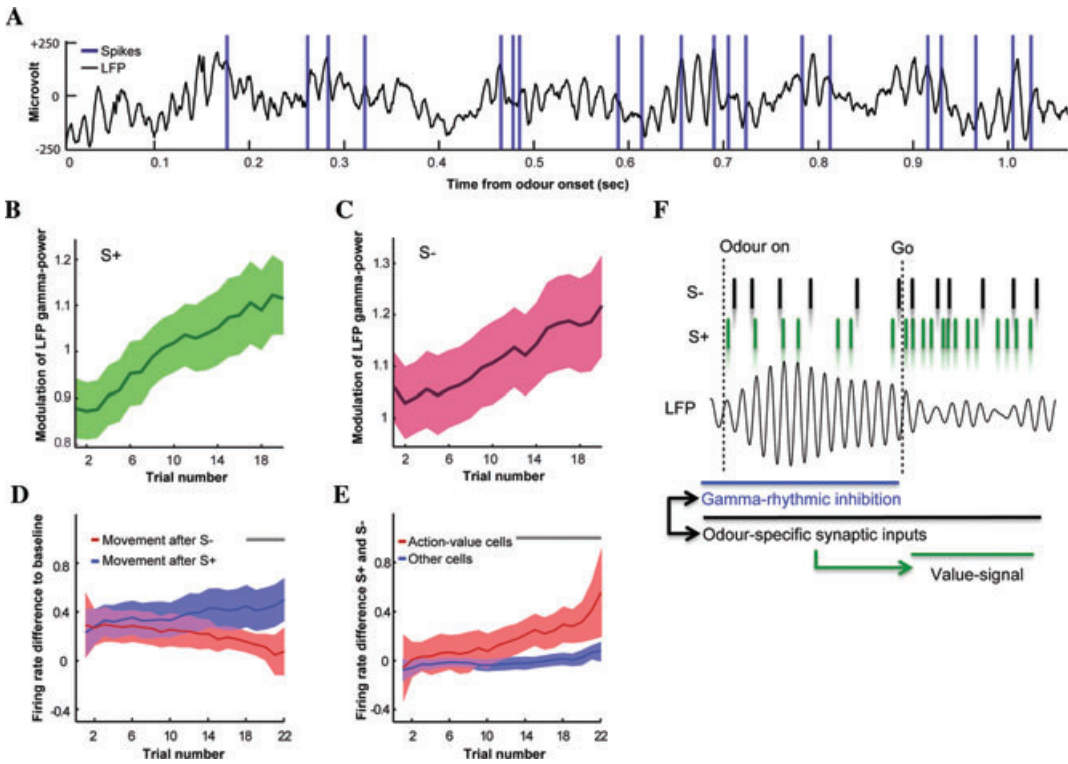


Figure 3. Gamma-band oscillations in the OFC. (A) Local field potential trace (black line, LFP) recorded from the OFC in a single trial, as a function of time from odor onset, together with spikes from an OFC neuron (blue, vertical lines). Note that the voltage scale on the y-axis does not correspond to the actual voltage scale of the spikes. Spikes tend to fall at the peak of gamma oscillations. (B) Average ratio of LFP gamma-power (60 Hz) during the S^+ odor period relative to baseline gamma power, as a function of trial number. A value of 1 indicates equal power. Shadings indicate a 95% confidence level, based on intersession variance. Gamma-band power increases linearly with time and is absent in the first few trials. (C) Same as for B, but now for the S^- odor. Note that the first 10 trials of a session were always S^+ trials, which may explain the higher starting value for the S^- condition. (D) Z-score standardized difference in action-value cell firing rates between the movement period and the baseline period, separate for the S^- (red) and S^+ condition (blue). Shadings indicate 95% confidence interval, based on intercell variance. Action value cell firing in the movement period becomes more discriminative over time. Gray horizontal bar denotes trials with a significant difference ($P < 0.01$, Mann–Whitney U test) between S^- and S^+ firing. (E) Z-score standardized difference in firing rates between the S^- and S^+ condition, separate for action-value cells (red) and other cells (blue). Plotting conventions are as in D. Action-value cell firing in the movement period becomes more discriminative over time, but the firing of other cell types does not. (F) Schematic illustration of the relationship between gamma-band oscillations and spiking activity. During odor stimulation (starting at “Odor on”), action value cells engage in strong gamma-band synchronization, and spikes tend to fall at the peak of the LFP gamma-band oscillation, which was simulated as filtered Gaussian white noise. However, cells do not discriminate in this phase between the S^+ and the S^- odor. This may be caused by gamma oscillatory activity, which causes a suppression of spiking activity. After termination of the obligatory odor sampling period (at “Go”), neurons are released from gamma-band synchronization and engage in desynchronized, value-selective activity, with typically higher firing rates for the S^+ condition (see D). Adapted from Van Wingerden *et al.*¹¹⁰

olfactory stimulation-induced theta band (8–10 Hz) but not gamma-band synchronization.

Surprisingly, gamma-band synchronization was predominantly expressed by a class of neurons (“action-value cells”) showing firing rate modulation after olfactory stimulation ceased, that is, when the rat moved toward the fluid well (Fig. 3D and E). Early in the session, the firing rate of these cells

in the movement period did not carry information about the outcome value associated with an olfactory stimulus. However, over the course of trials it became increasingly informative about outcome value (Fig. 3D), suggesting that these cells play a role in the acquisition of stimulus–outcome associations and in maintaining value representations during ongoing action patterns.

To elucidate how different OFC cell types contribute to local gamma-band synchronization, we compared the phase and strength of gamma-band synchronization between putative fast spiking basket cells and pyramidal cells. The separation of these two cell classes was based on characteristic features of the action potential waveform. To compare the strength of gamma-band synchronization between these two cell types, we removed any potential negative bias that could arise from the high firing rates of putative fast spiking basket cells.⁵⁰ Similar to Tukker *et al.*,¹¹⁷ but in contrast to Csicsvari *et al.*,¹¹⁸ we found that the strength of gamma-band synchronization did not differ between putative fast spiking basket cells and pyramidal cells. In fact, our “action-value cells” (which were characterized as putative pyramidal cells by large majority) were on average more gamma-band synchronized than the putative fast spiking basket cells. However, putative fast spiking basket cells with especially high firing rates were strongly gamma-band synchronized, suggesting that this subset of cells may rhythmically entrain the pyramidal cell population. In addition, we observed that fast spiking cells fired with a characteristic delay of $\sim 40^\circ$ relative to pyramidal cells, consistent with previous findings,^{117–119} suggesting that OFC gamma-band synchronization results from a temporal interplay between pyramidal cells and fast spiking basket cells. To summarize, although the OFC gamma rhythm is induced by the presentation of a sensory stimulus, it differs in several ways from the classic example of gamma-band synchronization in visual cortex,^{82,98,113,114,120–122} because it is learning-dependent but not stimulus-selective, and is expressed by a subclass of cells whose firing rate is inversely related to the strength of gamma-band synchronization. The induced OFC gamma-band synchronization is more similar to gamma-band synchronization found in the motor cortex, where it precedes motor execution,^{86,123} and where large, often positive, firing rate changes occur during the movement execution phase. In general, two types of relationships exist between the strength of gamma-band synchronization and the firing rate: first, a positive correlation, found, for example, in the visual cortex,^{81,82,113,114,121} and second, a negative correlation found in several nodes of the frontal cortex, namely the OFC, the motor cortex,¹²³ and the lateral prefrontal cortex.⁹⁶ However, a negative relationship may also be observed in V1 if surround

inhibition is the main factor controlling the firing rate.^{120,124} We propose that it is the balance between excitation and inhibition that determines whether a positive or a negative relationship arises. If excitation and inhibition increase in a balanced way, then both the firing rate and the strength of gamma-band synchronization increase.^{113,114} If, however, the proportion of inhibition increases in order to suppress firing rates, then the strength of gamma-band synchronization can increase concurrently. Inhibitory control over firing rates is important when execution of a movement or action-value representations needs to be inhibited, and needs to be matched to excitatory drive received in the preparatory (i.e., odor) phase. Gamma-band synchronization may arise as a by-product of this inhibitory suppression, due to the propensity of the fast spiking basket cells to engage in gamma-rhythmic activity. However, gamma-band synchronization may have an additional function by suppressing the firing rates in a controlled fashion by reducing the firing rate variance.¹²⁵ Preparatory gamma-band synchronization may also play an active role in priming movement or action-value cells and bringing them in a semiexcited, “idling” state.^{25,108,126} Thus, a more functional interpretation of gamma-band synchronization is not excluded.

Conclusions

Here, we reviewed two core aspects of neural coding in orbitofrontal cortex: the nature of population coding (especially considered in relation to future reward probability), and the dynamic organization of firing activity. As regards population coding, a first key feature is that subsets of OFC neurons “tessellate” all temporal phases of a task. In addition, they provide information anticipating upcoming events in the task, such as when neurons increase their firing rate already in advance of odor delivery at the onset of a trial.^{22,23} Neural coding of probability occurs during at least several phases, not as a distinct firing-rate signal of dedicated neurons, but rather as a rate modulation superimposed on the temporal task-coding structure. This pattern of superimposed modulation was previously also found for another outcome parameter, reward magnitude.²³ Both at the single-unit and population level, we found evidence for coding of reward probability, but not of uncertainty—a finding that may relate to the fact that rats in our task learned novel

stimulus–outcome contingencies every new session. In addition, coding at the population level appears to be distributed and redundant, both for reward probability and magnitude (see Ref. 23). Thus, many OFC neurons contribute individual “bits and pieces” to an overall matrix of encoded outcome parameters laid out according to the temporal structure of the task.

In addition to firing-rate coding, we found evidence for temporal coding of outcome-relevant information. First, highly synchronized spiking activity in the theta band occurred selectively during reward anticipation, and not in advance of an aversive outcome or during other task components such as locomotion or reward consumption. Considering the temporal shifting of theta power and spike-field phase locking during unexpected changes in outcome, phase-locked theta activity qualifies as a candidate mechanism for implementing a sustained value signal, as predicted by temporal difference learning models. Regardless of its function in error-driven reinforcement learning, theta-band synchrony may also function in regulating the efficiency with which orbitofrontal output affects target structures, such as the striatum, amygdala and higher associational cortices, and sculpts synaptic plasticity in these areas.

Second, coming back to the role of OFC gamma activity in relation to behavioral inhibition,¹⁶ it is striking that the OFC cells accounting for most of the gamma-band synchrony during the odor sampling phase were movement-related, action-value coding cells. We propose that, once the animal has identified a positive odor (S+) but is still required to maintain its poking posture, these movement-related cells are “kept on a leash” by the gamma oscillations to prevent them from becoming active prematurely. Once the required odor-sampling time window is over, these cells do become highly active, as evident from their average firing rate. This gamma-band oscillatory suppression may be a general mechanism that operates in a distributed manner across the prefrontal (or even frontal) cortex. When the OFC is lesioned, deficits in behavioral inhibition may or may not be seen, depending on the nature of the task and its dependence on different prefrontal areas.^{14,15,17} Various nonorbital prefrontal areas may, for instance, regulate the timing of behavioral responses in a way that is redundant with OFC control mechanisms. The action-suppression mecha-

nism indicated here for rat OFC may well operate in other PFC areas as well, which needs to be examined in future experiments. Clinically, a disruption of these mechanisms may account for disinhibitory features characteristic of obsessive-compulsive disorder and related conditions, such as attention-deficit hyperactivity disorder and Tourette’s syndrome.¹⁴

Conflicts of interest

The authors declare no conflicts of interest.

References

1. Baxter, M.G. *et al.* 2000. Control of response selection by reinforcer value requires interaction of amygdala and orbital prefrontal cortex. *J. Neurosci.* **20**: 4311–4319.
2. Bechara, A. *et al.* 1997. Deciding advantageously before knowing the advantageous strategy. *Science* **275**: 1293–1295.
3. Schoenbaum, G. *et al.* 2009. A new perspective on the role of the orbitofrontal cortex in adaptive behaviour. *Nat. Rev. Neurosci.* **10**: 885–892.
4. Tremblay, L. & W. Schultz. 1999. Relative reward preference in primate orbitofrontal cortex. *Nature* **398**: 704–708.
5. Groenewegen, H.J. & H.B. Uylings. 2000. The prefrontal cortex and the integration of sensory, limbic and autonomic information. *Prog. Brain Res.* **126**: 3–28.
6. Salzman, C.D. & S. Fusi. 2010. Emotion, cognition, and mental state representation in amygdala and prefrontal cortex. *Annu. Rev. Neurosci.* **33**: 173–202.
7. Burke, K.A. *et al.* 2009. Orbitofrontal inactivation impairs reversal of Pavlovian learning by interfering with ‘disinhibition’ of responding for previously unrewarded cues. *Eur. J. Neurosci.* **30**: 1941–1946.
8. De Bruin, J.P. *et al.* 2000. Role of the prefrontal cortex of the rat in learning and decision making: effects of transient inactivation. *Prog. Brain Res.* **126**: 103–113.
9. Dias, R., T.W. Robbins & A.C. Roberts. 1996. Dissociation in prefrontal cortex of affective and attentional shifts. *Nature* **380**: 69–72.
10. Pickens, C.L. *et al.* 2005. Orbitofrontal lesions impair use of cue–outcome associations in a devaluation task. *Behav. Neurosci.* **119**: 317–322.
11. Pickens, C.L. *et al.* 2003. Different roles for orbitofrontal cortex and basolateral amygdala in a reinforcer devaluation task. *J. Neurosci.* **23**: 11078–11084.
12. Stalnaker, T.A. *et al.* 2007. Basolateral amygdala lesions abolish orbitofrontal-dependent reversal impairments. *Neuron* **54**: 51–58.
13. Walton, M.E. *et al.* 2010. Separable learning systems in the macaque brain and the role of orbitofrontal cortex in contingent learning. *Neuron* **65**: 927–939.
14. Chamberlain, S.R. *et al.* 2005. The neuropsychology of obsessive compulsive disorder: the importance of failures in cognitive and behavioural inhibition as candidate endophenotypic markers. *Neurosci. Biobehav. Rev.* **29**: 399–419.

15. Chudasama, Y., J.D. Kralik & E.A. Murray. 2007. Rhesus monkeys with orbital prefrontal cortex lesions can learn to inhibit prepotent responses in the reversed reward contingency task. *Cereb. Cortex* **17**: 1154–1159.
16. Fuster, J.M. 2001. The prefrontal cortex—an update: time is of the essence. *Neuron* **30**: 319–333.
17. Man, M.S., H.F. Clarke & A.C. Roberts. 2009. The role of the orbitofrontal cortex and medial striatum in the regulation of prepotent responses to food rewards. *Cereb. Cortex* **19**: 899–906.
18. Kennerley, S.W. & J.D. Wallis. 2009. Evaluating choices by single neurons in the frontal lobe: outcome value encoded across multiple decision variables. *Eur. J. Neurosci.* **29**: 2061–2073.
19. Padoa-Schioppa, C. 2011. Neurobiology of economic choice: a good-based model. *Annu. Rev. Neurosci.* **34**: 333–359.
20. Padoa-Schioppa, C. & J.A. Assad. 2006. Neurons in the orbitofrontal cortex encode economic value. *Nature* **441**: 223–226.
21. Roesch, M.R., A.R. Taylor & G. Schoenbaum. 2006. Encoding of time-discounted rewards in orbitofrontal cortex is independent of value representation. *Neuron* **51**: 509–520.
22. van Duuren, E. *et al.* 2007. Neural coding of reward magnitude in the orbitofrontal cortex of the rat during a five-odor olfactory discrimination task. *Learn Mem.* **14**: 446–456.
23. van Duuren, E., J. Lankelma & C.M.A. Pennartz. 2008. Population coding of reward magnitude in the orbitofrontal cortex of the rat. *J. Neurosci.* **28**: 8590–8603.
24. Hsu, M. *et al.* 2005. Neural systems responding to degrees of uncertainty in human decision-making. *Science* **310**: 1680–1683.
25. Fries, P. 2005. A mechanism for cognitive dynamics: neuronal communication through neuronal coherence. *Trends Cogn. Sci.* **9**: 474–480.
26. Womelsdorf, T. *et al.* 2007. Modulation of neuronal interactions through neuronal synchronization. *Science* **316**: 1609–1612.
27. Abbott, L.F. & S.B. Nelson. 2000. Synaptic plasticity: taming the beast. *Nat. Neurosci.* **3**(Suppl): 1178–1183.
28. Paxinos, G. & C. Watson. 2007. *The Rat Brain in Stereotaxic Coordinates*. Academic Press/Elsevier. Amsterdam, Boston.
29. Lansink, C.S. *et al.* 2007. A split microdrive for simultaneous multi-electrode recordings from two brain areas in awake small animals. *J. Neurosci. Methods* **162**: 129–138.
30. Wilson, M.A. & B.L. McNaughton. 1993. Dynamics of the hippocampal ensemble code for space. *Science* **261**: 1055–1058.
31. Eichenbaum, H., R.A. Clegg & A. Feeley. 1983. Reexamination of functional subdivisions of the rodent prefrontal cortex. *Exp. Neurol.* **79**: 434–451.
32. Schoenbaum, G., A.A. Chiba & M. Gallagher. 1998. Orbitofrontal cortex and basolateral amygdala encode expected outcomes during learning. *Nat. Neurosci.* **1**: 155–159.
33. van Duuren, E. *et al.* 2009. Single-cell and population coding of expected reward probability in the orbitofrontal cortex of the rat. *J. Neurosci.* **29**: 8965–8976.
34. Hollerman, J.R., L. Tremblay & W. Schultz. 2000. Involvement of basal ganglia and orbitofrontal cortex in goal-directed behavior. *Prog. Brain Res.* **126**: 193–215.
35. van Duuren, E. *et al.* 2007. Pharmacological manipulation of neuronal ensemble activity by reverse microdialysis in freely moving rats: a comparative study of the effects of tetrodotoxin, lidocaine, and muscimol. *J. Pharmacol. Exp. Ther.* **323**: 61–69.
36. Zhang, K. *et al.* 1998. Interpreting neuronal population activity by reconstruction: unified framework with application to hippocampal place cells. *J. Neurophysiol.* **79**: 1017–1044.
37. Kepecs, A. *et al.* 2008. Neural correlates, computation and behavioural impact of decision confidence. *Nature* **455**: 227–231.
38. O'Neill, M. & W. Schultz. 2010. Coding of reward risk by orbitofrontal neurons is mostly distinct from coding of reward value. *Neuron* **68**: 789–800.
39. Carmichael, S.T. & J.L. Price. 1995. Limbic connections of the orbital and medial prefrontal cortex in macaque monkeys. *J. Comp. Neurol.* **363**: 615–641.
40. Cavada, C. *et al.* 2000. The anatomical connections of the macaque monkey orbitofrontal cortex. A review. *Cereb. Cortex* **10**: 220–242.
41. Hare, T.A. *et al.* 2008. Dissociating the role of the orbitofrontal cortex and the striatum in the computation of goal values and prediction errors. *J. Neurosci.* **28**: 5623–5630.
42. Rolls, E.T., C. McCabe & J. Redoute. 2008. Expected value, reward outcome, and temporal difference error representations in a probabilistic decision task. *Cereb. Cortex* **18**: 652–663.
43. Takahashi, Y.K. *et al.* 2009. The orbitofrontal cortex and ventral tegmental area are necessary for learning from unexpected outcomes. *Neuron* **62**: 269–280.
44. Rescorla, R.A. & A.R. Wagner. 1972. A theory of Pavlovian conditioning: variations in the effectiveness of reinforcement and nonreinforcement. In *Classical Conditioning II: Current Research and Theory*. Black, A.H. & W.F. Prokasy, Eds.: 64–99. Appleton-Century-Crofts. New York.
45. Sul, J.H. *et al.* 2010. Distinct roles of rodent orbitofrontal and medial prefrontal cortex in decision making. *Neuron* **66**: 449–460.
46. Sutton, R.S. & A.G. Barto. 1998. *Reinforcement Learning: An Introduction*. MIT Press. Cambridge, MA.
47. Pennartz, C.M.A. *et al.* 2011. The hippocampal-striatal axis in learning, prediction and goal-directed behavior. *Trends Neurosci.* **34**: 548–559.
48. Pennartz, C.M.A. 1997. Reinforcement learning by Hebbian synapses with adaptive thresholds. *Neuroscience* **81**: 303–319.
49. Pennartz, C., B. McNaughton & A.B. Mulder. 2000. The glutamate hypothesis of reinforcement learning. In *Cognition, Emotion and Autonomic Responses: The Integrative Role of the Prefrontal Cortex and Limbic Structures*. Uylings, H.B. *et al.*, Eds.: 231–253. Elsevier, Ltd. Amsterdam, the Netherlands.
50. Schroeder, C.E. & P. Lakatos. 2009. Low-frequency neuronal oscillations as instruments of sensory selection. *Trends Neurosci.* **32**: 9–18.
51. DeCoteau, W.E. *et al.* 2007. Learning-related coordination of striatal and hippocampal theta rhythms during

- acquisition of a procedural maze task. *Proc. Natl. Acad. Sci. USA* **104**: 5644–5649.
52. Paz, R., E.P. Bauer & D. Paré. 2008. Theta synchronizes the activity of medial prefrontal neurons during learning. *Learn Mem.* **15**: 524–531.
 53. Siapas, A.G., E.V. Lubenov & M.A. Wilson. 2005. Prefrontal phase locking to hippocampal theta oscillations. *Neuron* **46**: 141–151.
 54. Buzsáki, G. 2006. *Rhythms of the Brain*. Oxford University Press, Oxford, New York.
 55. Pesaran, B., M.J. Nelson & R.A. Andersen. 2008. Free choice activates a decision circuit between frontal and parietal cortex. *Nature* **453**: 406–409.
 56. Benchenane, K. *et al.* 2010. Coherent theta oscillations and reorganization of spike timing in the hippocampal-prefrontal network upon learning. *Neuron* **66**: 921–936.
 57. Wang, X.J. 2010. Neurophysiological and computational principles of cortical rhythms in cognition. *Physiol. Rev.* **90**: 1195–1268.
 58. Womelsdorf, T. *et al.* 2010. Theta-activity in anterior cingulate cortex predicts task rules and their adjustments following errors. *Proc. Natl. Acad. Sci. USA* **107**: 5248–5253.
 59. Womelsdorf, T. *et al.* 2010. Selective theta-synchronization of choice-relevant information subserves goal-directed behavior. *Front. Hum. Neurosci.* **4**: 1–13. Article 210.
 60. Buzsáki, G. 2005. Theta rhythm of navigation: link between path integration and landmark navigation, episodic and semantic memory. *Hippocampus* **15**: 827–840.
 61. Battaglia, F. *et al.* 2011. The hippocampus: memory hub for communication in brain networks. *Trends Cogn. Sci.* **15**: 310–318.
 62. van Wingerden, M. *et al.* 2010. Theta-band phase locking of orbitofrontal neurons during reward expectancy. *J. Neurosci.* **30**: 7078–7087.
 63. Vinck, M. *et al.* 2011. An improved index of phase-synchronization for electrophysiological data in the presence of volume-conduction, noise and sample-size bias. *Neuroimage* **55**: 1548–1565.
 64. Vinck, M. *et al.* 2010. The pairwise phase consistency: a bias-free measure of rhythmic neuronal synchronization. *Neuroimage* **51**: 112–122.
 65. Gutierrez, R., S.A. Simon & M.A. Nicolelis. 2010. Licking-induced synchrony in the taste-reward circuit improves cue discrimination during learning. *J. Neurosci.* **30**: 287–303.
 66. Schultz, W., P. Dayan & P.R. Montague. 1997. A neural substrate of prediction and reward. *Science* **275**: 1593–1599.
 67. Niv, Y. & G. Schoenbaum. 2008. Dialogues on prediction errors. *Trends Cogn. Sci.* **12**: 265–272.
 68. Lansink, C.S. *et al.* 2009. Hippocampus leads ventral striatum in replay of place-reward information. *PLoS Biol.* **7**: 1–11.
 69. Seidenbecher, T. *et al.* 2003. Amygdalar and hippocampal theta rhythm synchronization during fear memory retrieval. *Science* **301**: 846–850.
 70. Lisman, J. 2005. The theta/gamma discrete phase code occurring during the hippocampal phase precession may be a more general brain coding scheme. *Hippocampus* **15**: 913–922.
 71. Bi, G.-q. & M.-m. Poo. 1998. Synaptic modifications in cultured hippocampal neurons: dependence on spike timing, synaptic strength, and postsynaptic cell type. *J. Neurosci.* **18**: 10464–10472.
 72. Cassenaer, S. & G. Laurent. 2007. Hebbian STDP in mushroom bodies facilitates the synchronous flow of olfactory information in locusts. *Nature* **448**: 709–713.
 73. Canolty, R.T. *et al.* 2006. High gamma power is phase-locked to theta oscillations in human neocortex. *Science* **313**: 1626–1628.
 74. Tort, A.B. *et al.* 2008. Dynamic cross-frequency couplings of local field potential oscillations in rat striatum and hippocampus during performance of a T-maze task. *Proc. Natl. Acad. Sci. USA* **105**: 20517–20522.
 75. Canolty, R.T. & R.T. Knight. 2010. The functional role of cross-frequency coupling. *Trends Cogn. Sci.* **14**: 506–515.
 76. Bauer, M. *et al.* 2006. Tactile spatial attention enhances gamma-band activity in somatosensory cortex and reduces low-frequency activity in parieto-occipital areas. *J. Neurosci.* **26**: 490–501.
 77. Bragin, A. *et al.* 1995. Gamma (40–100 Hz) oscillation in the hippocampus of the behaving rat. *J. Neurosci.* **15**: 47–60.
 78. Brosch, M., E. Budinger & H. Scheich. 2002. Stimulus-related gamma oscillations in primate auditory cortex. *J. Neurophysiol.* **87**: 2715–2725.
 79. Cardin, J.A. *et al.* 2009. Driving fast-spiking cells induces gamma rhythm and controls sensory responses. *Nature* **459**: 663–667.
 80. Eeckman, F.H. & W.J. Freeman. 1990. Correlations between unit firing and EEG in the rat olfactory system. *Brain Res.* **528**: 238–244.
 81. Fries, P. *et al.* 2001. Modulation of oscillatory neuronal synchronization by selective visual attention. *Science* **291**: 1560–1563.
 82. Gray, C.M. *et al.* 1989. Oscillatory responses in cat visual cortex exhibit inter-columnar synchronization which reflects global stimulus properties. *Nature* **338**: 334–337.
 83. Kalenscher, T. *et al.* Reward-associated gamma oscillations in ventral striatum are regionally differentiated and modulate local firing activity. *J. Neurophysiol.* **103**: 1658–1672.
 84. Pesaran, B. *et al.* 2002. Temporal structure in neuronal activity during working memory in macaque parietal cortex. *Nat. Neurosci.* **5**: 805–811.
 85. van der Meer, M.A. & A.D. Redish. 2009. Low and high gamma oscillations in rat ventral striatum have distinct relationships to behavior, reward, and spiking activity on a learned spatial decision task. *Front. Integr. Neurosci.* **3**: 1–19. Article 9.
 86. Schoffelen, J.M., R. Oostenveld & P. Fries. 2005. Neuronal coherence as a mechanism of effective corticospinal interaction. *Science* **308**: 111–113.
 87. Wehr, M. & G. Laurent. 1996. Odour encoding by temporal sequences of firing in oscillating neural assemblies. *Nature* **384**: 162–166.
 88. Gregoriou, G.G. *et al.* 2009. High-frequency, long-range coupling between prefrontal and visual cortex during attention. *Science* **324**: 1207–1210.

89. Womelsdorf, T. *et al.* 2006. Gamma-band synchronization in visual cortex predicts speed of change detection. *Nature* **439**: 733–736.
90. Hoogenboom, N. *et al.* 2010. Visually induced gamma-band activity predicts speed of change detection in humans. *Neuroimage* **51**: 1162–1167.
91. Taylor, K. *et al.* 2005. Coherent oscillatory activity in monkey area v4 predicts successful allocation of attention. *Cereb. Cortex* **15**: 1424–1437.
92. de Almeida, L., M. Idiart & J.E. Lisman. 2009. A second function of gamma frequency oscillations: an E%-max winner-take-all mechanism selects which cells fire. *J. Neurosci.* **29**: 7497–7503.
93. Fries, P., D. Nikolic & W. Singer. 2007. The gamma cycle. *Trends Neurosci.* **30**: 309–316.
94. König, P. *et al.* 1995. How precise is neuronal synchronization? *Neural Comput.* **7**: 469–485.
95. Rotermund, D. *et al.* 2009. Attention improves object representation in visual cortical field potentials. *J. Neurosci.* **29**: 10120–10130.
96. Siegel, M., M.R. Warden & E.K. Miller. 2009. Phase-dependent neuronal coding of objects in short-term memory. *Proc. Natl. Acad. Sci. USA* **106**: 21341–21346.
97. Singer, W. 1999. Neuronal synchrony: a versatile code for the definition of relations? *Neuron* **24**: 49–65, 111–125.
98. Vinck, M. *et al.* 2010. Gamma-phase shifting in awake monkey visual cortex. *J. Neurosci.* **30**: 1250–1257.
99. Gulyás, A.I. *et al.* 2010. Parvalbumin-containing fast-spiking basket cells generate the field potential oscillations induced by cholinergic receptor activation in the hippocampus. *J. Neurosci.* **30**: 15134–15145.
100. Sohal, V.S. *et al.* 2009. Parvalbumin neurons and gamma rhythms enhance cortical circuit performance. *Nature* **459**: 698–702.
101. Tiesinga, P. & T.J. Sejnowski. 2009. Cortical enlightenment: are attentional gamma oscillations driven by ING or PING? *Neuron* **63**: 727–732.
102. Whittington, M.A. *et al.* 2011. Multiple origins of the cortical gamma rhythm. *Dev. Neurobiol.* **71**: 92–106.
103. Bartos, M., I. Vida & P. Jonas. 2007. Synaptic mechanisms of synchronized gamma oscillations in inhibitory interneuron networks. *Nat. Rev. Neurosci.* **8**: 45–56.
104. Cobb, S.R. *et al.* 1995. Synchronization of neuronal activity in hippocampus by individual GABAergic interneurons. *Nature* **378**: 75–78.
105. Whittington, M.A., R.D. Traub & J.G. Jefferys. 1995. Synchronized oscillations in interneuron networks driven by metabotropic glutamate receptor activation. *Nature* **373**: 612–615.
106. Wulff, P. *et al.* 2009. Hippocampal theta rhythm and its coupling with gamma oscillations require fast inhibition onto parvalbumin-positive interneurons. *Proc. Natl. Acad. Sci. USA* **106**: 3561–3566.
107. Beshel, J., N. Kopell & L. M. Kay. 2007. Olfactory bulb gamma oscillations are enhanced with task demands. *J. Neurosci.* **27**: 8358–8365.
108. Fries, P. *et al.* 2001. Rapid feature selective neuronal synchronization through correlated latency shifting. *Nat. Neurosci.* **4**: 194–200.
109. Kay, L.M. 2003. Two species of gamma oscillations in the olfactory bulb: dependence on behavioral state and synaptic interactions. *J. Integr. Neurosci.* **2**: 31–44.
110. van Wingerden, M. *et al.* 2010. Learning-associated gamma-band phase-locking of action-outcome selective neurons in orbitofrontal cortex. *J. Neurosci.* **30**: 10025–10038.
111. Hoogenboom, N. *et al.* 2006. Localizing human visual gamma-band activity in frequency, time and space. *Neuroimage* **29**: 764–773.
112. Zhou, Z., M.R. Bernard & A.B. Bonds. 2008. Deconstruction of spatial integrity in visual stimulus detected by modulation of synchronized activity in cat visual cortex. *J. Neurosci.* **28**: 3759–3768.
113. Friedman-Hill, S., P.E. Maldonado & C.M. Gray. 2000. Dynamics of striate cortical activity in the alert macaque: I. Incidence and stimulus-dependence of gamma-band neuronal oscillations. *Cereb. Cortex* **10**: 1105–1116.
114. Henrie, J.A. & R. Shapley. 2005. LFP power spectra in V1 cortex: the graded effect of stimulus contrast. *J. Neurophysiol.* **94**: 479–490.
115. Lima, B. *et al.* 2010. Synchronization dynamics in response to plaid stimuli in monkey V1. *Cereb. Cortex.* **20**: 1556–1573.
116. Liu, J. & W.T. Newsome. 2006. Local field potential in cortical area MT: stimulus tuning and behavioral correlations. *J. Neurosci.* **26**: 7779–7790.
117. Tukker, J.J. *et al.* 2007. Cell type-specific tuning of hippocampal interneuron firing during gamma oscillations in vivo. *J. Neurosci.* **27**: 8184–8189.
118. Csicsvari, J. *et al.* 2003. Mechanisms of gamma oscillations in the hippocampus of the behaving rat. *Neuron* **37**: 311–322.
119. Hasenstaub, A. *et al.* 2005. Inhibitory postsynaptic potentials carry synchronized frequency information in active cortical networks. *Neuron* **47**: 423–435.
120. Gieselmann, M.A. & A. Thiele. 2008. Comparison of spatial integration and surround suppression characteristics in spiking activity and the local field potential in macaque V1. *Eur. J. Neurosci.* **28**: 447–459.
121. Ray, S. & J.H. Maunsell. 2010. Differences in gamma frequencies across visual cortex restrict their possible use in computation. *Neuron* **67**: 885–896.
122. Siegel, M. & P. König. 2003. A functional gamma-band defined by stimulus-dependent synchronization in area 18 of awake behaving cats. *J. Neurosci.* **23**: 4251–4260.
123. Donoghue, J.P. *et al.* 1998. Neural discharge and local field potential oscillations in primate motor cortex during voluntary movements. *J. Neurophysiol.* **79**: 159–173.
124. Chalk, M. *et al.* 2010. Attention reduces stimulus-driven gamma frequency oscillations and spike field coherence in V1. *Neuron* **66**: 114–125.
125. Mitchell, J.F., K.A. Sundberg & J.H. Reynolds. 2009. Spatial attention decorrelates intrinsic activity fluctuations in macaque area V4. *Neuron* **63**: 879–888.
126. Briggs, F. & W.M. Usrey. 2007. Cortical activity influences geniculocortical spike efficacy in the macaque monkey. *Front. Integr. Neurosci.* **1**: 1–5. Article 3.